Near-Field Acoustic Holography of a Vibrating Drum Head

Brendan Sullivan
University of Illinois at Urbana-Champaign

Dec. 18, 2008

ABSTRACT

This paper explains the design and construction of a phase-sensitive near-field acoustic holography apparatus. By using phase-sensitive lock-in amplifier techniques to record the complex signals of pressure and particle velocity microphones over an extended spatial region, small vibrations can be imaged using the acoustical properties of said vibrations. The apparatus is tested on a vibrating drumhead and the first few eigenmodes are visualized.

Introduction

Acoustic holography is a method of imaging that uses the acoustic properties of a vibrating object to create an image of a system. Just as an atomic force microscope works by measuring the vibrations of a cantilever, acoustic holography uses microphones to record the pressure (p) and particle velocity (u) over a region of space and, in doing so, permits graphical representation either of an objects's vibrations or its associated sound-field. Acoustic holography has a wide array of applications, ranging from speaker design to measuring acoustic radiation of an arbitrary object, as Ref. [1] shows. This paper discusses a phase-sensitive method for measuring the complex pressure ($\tilde{p}$) and particle velocity ($\tilde{u}$) over a surface or volume to reconstruct and analyze the complex sound field produced from an arbitrary sound source. This method uses tiny pressure and particle velocity microphones attached to an x-y translation stage along which the microphones can be moved small distances. Recording the complex pressure and particle velocity over an appropriate spatial range permits an image to be created of an arbitrary vibrating object.

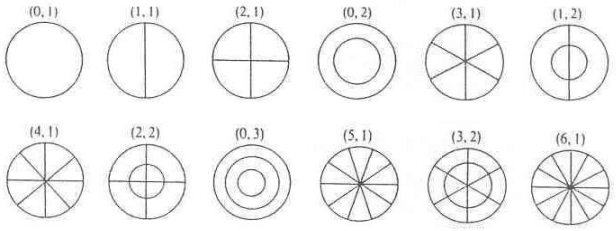

Fig. 1: The first 12 eigenmodes of a drumhead. Adjacent regions oscillate out of phase. For instance, in mode (0,1) the entire drum head moves in phase while in mode (1,1) the left and right side of the drumhead are 180° out of phase. Image modified from Ref. [2].

A vibrating drumhead was chosen to test the apparatus. A drumhead is effectively a membrane with clamped-edge boundary conditions, the theory for which can be found in [2]. When a drumhead resonates, its motion corresponds to superposition of its eigenmodes (the first twelve of which are shown in Fig. 1). By exciting the drumhead at an eigenfrequency corresponding to an eigenmode, it is possible to directly observe each eigenmode and image the motion of air in proximity to the drumhead.

Drumheads are not the only system this apparatus can measure. Measurements may be made along different directions, allowing measurement of any arbitrary sound field. Another natural candidate for testing with this apparatus, perhaps because of its similarities to a drumhead, is a cymbal. It has been verified using optical holography that the eigenmodes of a cymbal form fractals [3]. The fractal nature of a cymbal's eigenmodes should be observable using the same method as is used to observe the eigenmodes of a drumhead. Additionally, this method could be expanded to very accurately measure an arbitrary sound field, for instance the near and far-field acoustic radiation from a loudspeaker.

In addition to offering the first phase-sensitive measurements of this kind, the microphones associated with this apparatus can be placed much closer to the object. Typically measurements of this sort are taken with a large array of microphones which effectively creates a surface above the object. Placing this surface in proximity to the vibrating object can profoundly change the resulting sound field, similar to the casing around speakers. Because the apparatus described below uses a single pair of very compact microphones, they can be placed within a few millimeters of a vibrating object without substantial sound field interference. Furthermore, it has been shown [4,5] that for a

planar object such as a drumhead that the sound field near the vibrating surface can be related to the sound field at the vibrating surface. For a microphone located at a height $h = z_m$ above source the plane can be described in the wave-number amplitude space. Using a standard fast Fourier transform (FFT):

$$\tilde{P}\left(k_x, k_y, z_m\right) = \int_{-\infty}^{+\infty}\int_{-\infty}^{+\infty} \tilde{p}\left(x, y, z_m\right) e^{i\left(k_x x + k_y y\right)} dxdy \equiv FFT\left\{\tilde{p}\left(x, y, z_m\right)\right\}$$

$$\tilde{U}_z\left(k_x, k_y, z_m\right) = \int_{-\infty}^{+\infty}\int_{-\infty}^{+\infty} \tilde{u}_z\left(x, y, z_m\right) e^{i\left(k_x x + k_y y\right)} dxdy \equiv FFT\left\{\tilde{u}_z\left(x, y, z_m\right)\right\}$$

Where $\tilde{p}$ and $\tilde{u}$ respectively represent pressure and the normal component of particle velocity recorded by the microphones. In wave-number (k) space, there are two regions of interest. Inside the radiation circle ($k_x^2 + k_y^2 \leq k$), the values of $\tilde{p}$ and $\tilde{u}$ are taken to be the amplitude of the respective wave. To mathematically translate the microphone from height $h = z_m$ to height $h = z_{surface}$, a propagator, $\tilde{G}$, is used:

$$\tilde{G}\left(z_p, z_m, k_x, k_y\right) \equiv e^{-ik_z\left(z_p - z_m\right)}$$

With ρ_0 the density of air, c the propagation speed of the wave, and Δz the microphones' distance from the vibrating surface.

Once this is complete, the complex pressure and particle velocity *at the vibrating surface* are given by the inverse FFT:

$$\tilde{p}\left(x, y, z_p\right) = FFT^{-1}\left\{\tilde{P}\left(k_x, k_y, z_p\right)\right\} = FFT^{-1}\left\{\tilde{G}\left(z_p, z_m, k_x, k_y\right)\tilde{P}\left(k_x, k_y, z_m\right)\right\}$$

$$\tilde{u}_z\left(x, y, z_p\right) = FFT^{-1}\left\{\tilde{U}_z\left(k_x, k_y, z_p\right)\right\} = FFT^{-1}\left\{\tilde{G}\left(z_p, z_m, k_x, k_y\right)\tilde{U}_z\left(k_x, k_y, z_m\right)\right\}$$

Since particle displacement (*i.e.,* the time integral of particle velocity, $\tilde{u}$) at the vibrating surface must be the same as the vibrating surface's displacement, the vibrating membrane can be imaged.

In addition to complex pressure, particle velocity, and displacement ($\tilde{p}$, $\tilde{u}$, and $\tilde{d}$, respectively), there are several other useful quantities to define. The simplest of these is

acceleration, the time derivative of particle velocity. The next is the longitudinal specific acoustic impedance, $\tilde{Z} = \tilde{p}/\tilde{u}$. The acoustic impedance is analogous to Ohm's Law (with units of acoustical Ohms) in electronics and is a property of the medium through which a sound wave is propagating. The final substantial physical quantity is the complex sound intensity, $\tilde{I} = \tilde{p} \times \tilde{u}^*$ which is related to energy flow and work done by the sound field. The units of $\tilde{I}$ are W / m^2.

The rest of this paper describes the apparatus in more detail. The results given and exact procedure are given for the study of drumhead motion, though this methodology could easily be used on any other vibrating object.

Apparatus and Procedures

In order to observe the normal modes of the drum, a mechanism must be used that allows precise spatial scanning of the drumhead. To achieve this, the microphones were attached to a set of motorized, high-precision Thompson rods (See Fig. 2). These translation stages are capable of accuracy within a micrometer of the desired position. The Thompson rods' motors are connected to a computerized data acquisition (DAQ) system. The microphones were held at a small distance $h = z_m$ above the drumhead and record the complex pressure and particle velocity. After a measurement was made at a particular x-y position, the DAQ system moved the microphones using the translation stages to the next position to be measured. By measuring in very small spatial intervals at the drumhead's resonances, the sound field immediately above the drumhead and consequently the motion of the drumhead, was obtained. To determine the

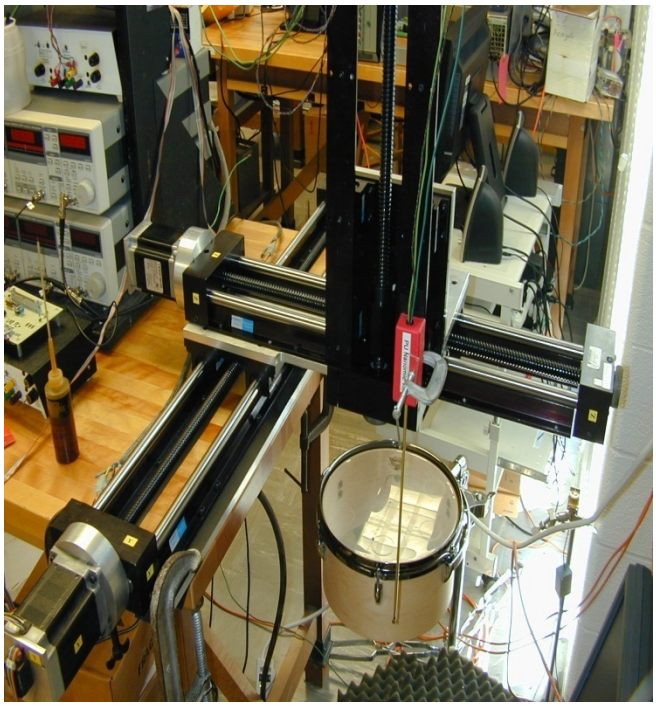

Figure 2a: The Thompson Rods form the three axes through which the microphone (red box) moves. The rods are controlled by the data acquisition system.

phase relative to the driving function generator, the complex signal of each microphone was read via a lock-in amplifier referenced to the function generator producing sine waves. A block diagram of this setup is shown in Fig. 2b.

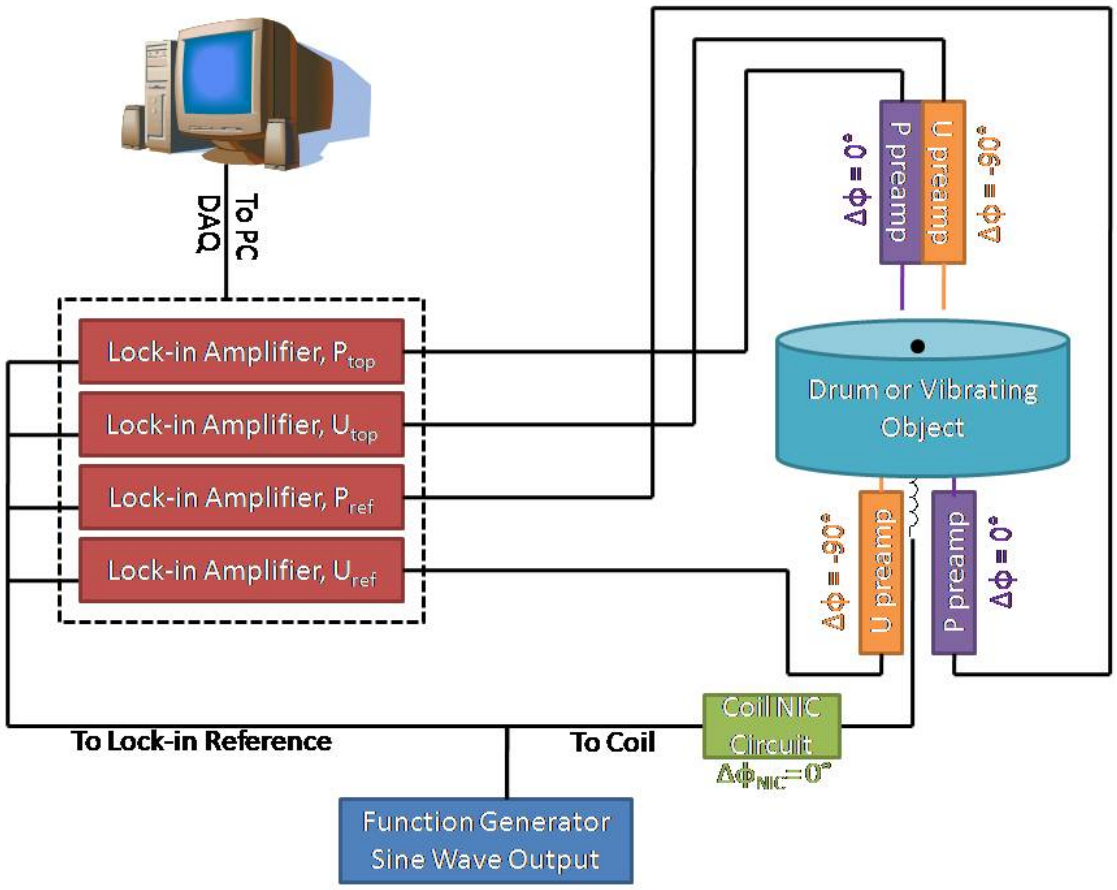

Figure 2b: A block diagram of the experiment with the electronics phase shift associated with each component. The magnets (black dot) are driven by the coil a la the NIC. The microphones under the drumhead are used to phase lock to a particular resonance while the top microphones are used to scan the drumhead in both the frequency and spatial scan modes.

Since this is a phase-sensitive measurement, caution was used in calibrating the microphones' phase. Electronically, this was done in the same fashion described in Ref. [7]. The distance from the microphones to the also drumhead introduces a frequency-dependent phase change, known as the propagation phase. The propagation phase can be found by holding the microphone at a constant position in space (x_0,y_0,z_0) near the drumhead and scanning frequency. Then, barring all resonances, the phase should be constant. It was observed that over the ~ 0 Hz to 1

kHz range, both p and u had about a 36° phase change that was nearly linear with frequency. This linear fit has been applied to the data given in this paper.

To extract physical quantities from the microphones, the microphones were absolutely calibrated. After absolute calibration, output voltage from the microphone could be related to either pressure or particle velocity, depending on the microphone. This was done using an Exetech calibrator, which produces a L_p = 94 dB sound field. By definition,

$$L_p = 20 \log\left(\frac{p_{sound}}{p_0}\right) = 94 \text{ dB}$$

with p_0 the pressure of free air, or $2 \times 10^{-5}\ N/m^2$ at normal temperature and pressure (NTP). From the above equation for L_p, it follows that the pressure of the sound field of 94 dB must correspond to a pressure of 1 Pa. From the Euler equation, it can also be shown that a 94 dB sound field corresponds to a particle velocity of 2.4 mm / s. By recording the output voltage of a microphone exposed to a 94 dB sound field and relating that to the associated pressure and particle velocity, the microphone values can be expressed in Pa or mm / s, rather than arbitrary volts.

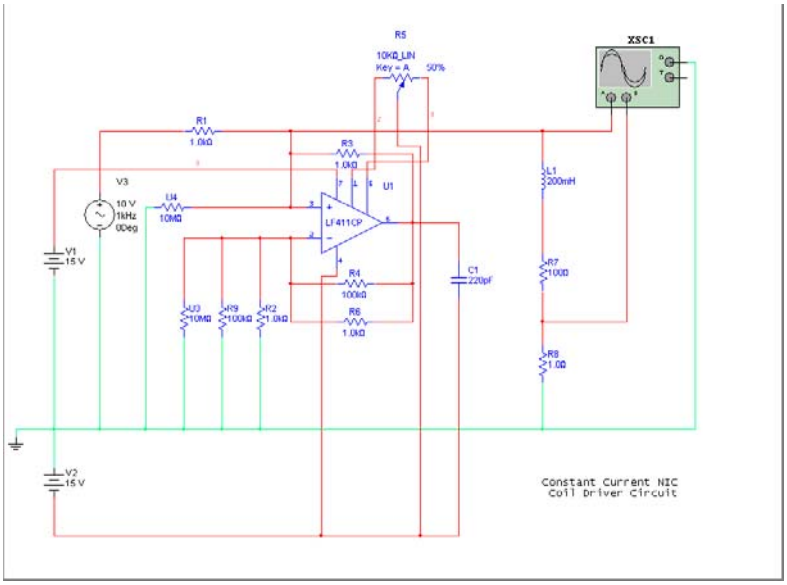

Figure 3: The constant current NIC for the driver coil. This circuit ensures that the magnets amplitude is constant.

To ensure that the amplitude of the magnetic field driving the drumhead was constant, a negative impedance circuit (NIC) constant current driver was placed between the function generator and coil. Since the magnetic field of the coil is linearly proportional to current through the coil, I, it had to be ensured that the current amplitude, not voltage, remained constant with frequency.

Figure 4 shows simulation data on the circuit's behavior. The branch \$10, shown in purple,

represents current amplitude through the coil. In the region of interest, f << 10 kHz, the coil's current exhibits flat response in both magnitude and phase, as is required of this circuit.

Because the location of the magnet is, by necessity, an anti-node on the drumhead, it's longitudinal motion can be modeled as a damped, driven harmonic oscillator with the equation of motion $m\ddot{\tilde{z}}+m\gamma\dot{\tilde{z}}+k\tilde{z}=F_{z,magnet}$. m here represents the mass of the magnets and drumhead clamped by the magnets, γ the drumhead's damping coefficient, and $F_{z,magnet}$ is the longitudinal component of force on the magnets from the coil. Treating the two magnets as a pure magnetic dipole with moment $\vec{m}_{mag}$, the force can be expressed as

$$\vec{F}_{mag}(\vec{r},t)=\vec{\nabla}\left[\vec{m}_{mag}(\vec{r})\bullet\vec{B}_{coil}(\vec{r},t)\right]=\vec{m}_{mag}(\vec{r})\bullet\vec{\nabla}\vec{B}_{coil}(\vec{r},t)+\vec{B}_{coil}(\vec{r},t)\bullet\vec{\nabla}\vec{m}_{mag}(\vec{r})$$
$$+\vec{m}_{mag}(\vec{r})\times\underbrace{\left(\vec{\nabla}\times\vec{B}_{coil}(\vec{r},t)\right)}_{=\frac{1}{c^2}\frac{\partial\vec{E}_{coil}(\vec{r},t)}{\partial t}}+\vec{B}_{coil}(\vec{r},t)\times\left(\vec{\nabla}\times\vec{m}_{mag}(\vec{r})\right)$$

Once the calibrated data was taken, a surface was drawn over spatial coordinates and various acoustical properties. This was done using an MATLAB m-file that first formed a mesh-grid of all the coordinates where data was taken and then plotted a three dimensional surface of the quantities measured. This surface, when measured at one of the drum's resonances, emulates the normal modes shown in the motivation section of this paper, confirming the experimental observation of the drum's eigenmodes.

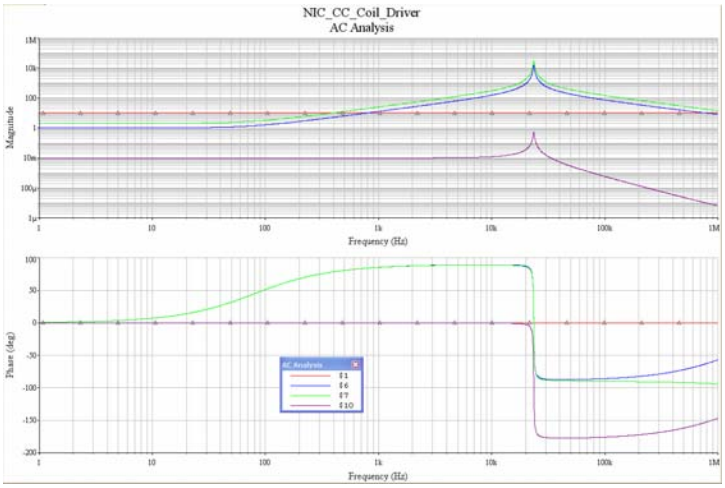

Figure 4: Frequency response of the NIC circuit. The current amplitude through the coil is given by $10, the purple line. In the region of interest (<<10 kHz) the response is flat in both magnitude and phase.

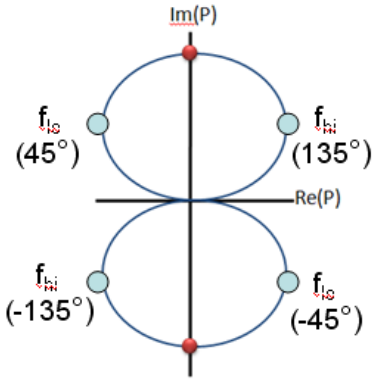

Figure 5: To compensate for the eigenfrequency drift due to temperature, the frequency is shifted between scanning points until pressure falls on one of the two red dots above.

Because resonances of drumheads have a strong temperature dependence, a mode-locking system had to be installed in the apparatus. When the drum is vibrating on an eigenmode, the pressure directly underneath the magnet will be extremal and entirely imaginary (one of the red dots in Fig. 5). Consequently, a pair of mode-locking pressure and particle velocity microphones were placed underneath the drumhead and the desired resonance was found. Ambient temperature drift lead to a drift in resonance frequency, so the excitation frequency was tweaked between scanning points until the imaginary component of pressure was at an extremal point, shown in Fig. 5. The frequency is set by hand to be between f_{lo} and f_{hi}. Then, between scanning points the frequency is tweaked, which effectively shifts the pressure along the blue curve in Fig. 5, until the resonance is found again (the red dot). It is worth noting that if the temperature changes too drastically or the mode-locking system overshoots its target by too much (*i.e.* goes beyond f_{lo} or f_{hi}) then the mode has been lost and the current scan must be discontinued. The typical variation is around $f_{hi} - f_{lo} = 1$ Hz.

Results and Analysis

The results of a typical axisymmetric frequency scan are given in Fig. 6. There are several noteworthy features in these plots. First, since this was taking with the microphones at the center of the drum, the first few peaks in each spectrum indicate the first few (0,n) modes. That is to say, the first peak in *p* represents the (0,1) mode as determined by *p*, the second peak is the (0,2) mode, and so on. Additionally for these peaks, the parities of pressure are all the same. For example, the real part of the pressure will fall before it hits a maximum, while the imaginary component is always

positive, and typically zero. This is convenient for programming the phase-lock loop because it ensures that the feedback can always use negative feedback with the same procedure. It may be the case with the non axisymmetric modes that the parity changes, in which case the parity will have to be manually entered for each mode. Finally, the phase of both *p* and *u* undergo a series of regular, sharp spikes. Examining the log plot of the phase (second in the right column of Fig. 6) makes it much clearer to see that the phase is constant at frequencies local to resonant peaks in their respective properties. This is because, near the resonant peak, the phase is dominated by the nearby mode. Far away from the resonant peaks, the microphone signal is dominated by the building's ventilation system.

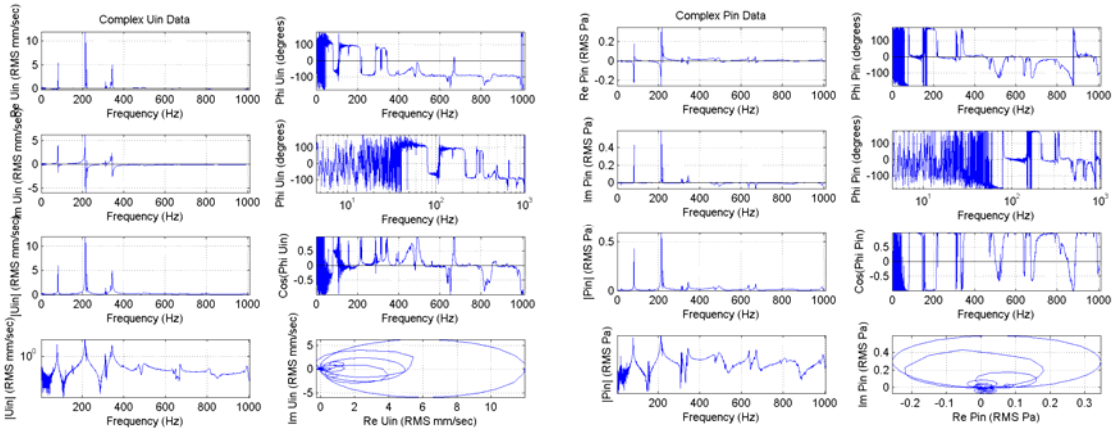

Figure 6: Complex *p* (right) and *u* (left) data taken at the center of the drum, $\rho = 0$. The first few peaks in the spectrum represent the first few axisymmetric, (0,n) modes.

The above frequency scans can be used to acquire a reasonable estimate of resonance locations. Because the temperature in the room may fluctuate after a peak is found, the peak location is not exact. Consequently, to perform a spatial scan after a frequency scan requires the use of the mode-locking system.

As mentioned before mentioned, the phase observed by the reference microphone should be a constant 90° or -90°. Figure 7 shows the reference phase as a function of measurement number. The phase is roughly locked at the desired -90°. To further demonstrate the effect of the mode-locking setup, the resonant frequency as a function of measurement number is given in Fig. 8.

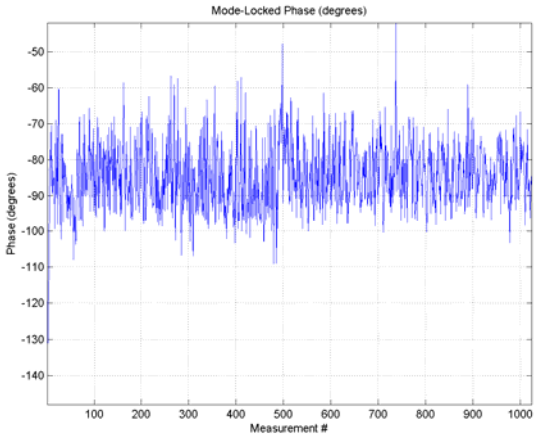

Figure 7: Reference phase versus measurement number. The reference phase is roughly a constant -90 except for the spikes to 0. These spikes are an artifact of the measurement, and represent the phase of free air (arbitrarily taken to be zero).

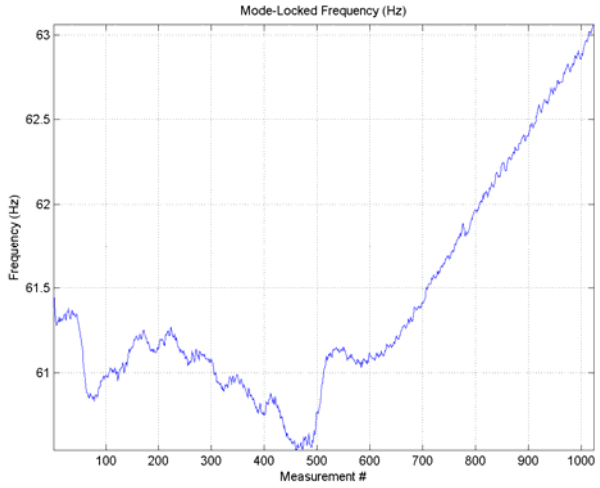

Figure 8: Sample frequency as a function of measurement number. In an ideal system the resonant frequency would be constant throughout the measurement. However, drifts in ambient temperature lead to drifts in resonant frequency.

In an ideal system, the frequency would be constant, and determined solely by the geometry of the system. However, temperature variations cause a drift in the resonant frequency of the drum.

A spatial scan of the drumhead unambiguously reveals the mode. Figure 9 shows data for the (0,1) resonance mode and Fig. 10 shows the (0,2) mode. Note that since Re(P) and Im(U) are zero across the head, they are omitted.

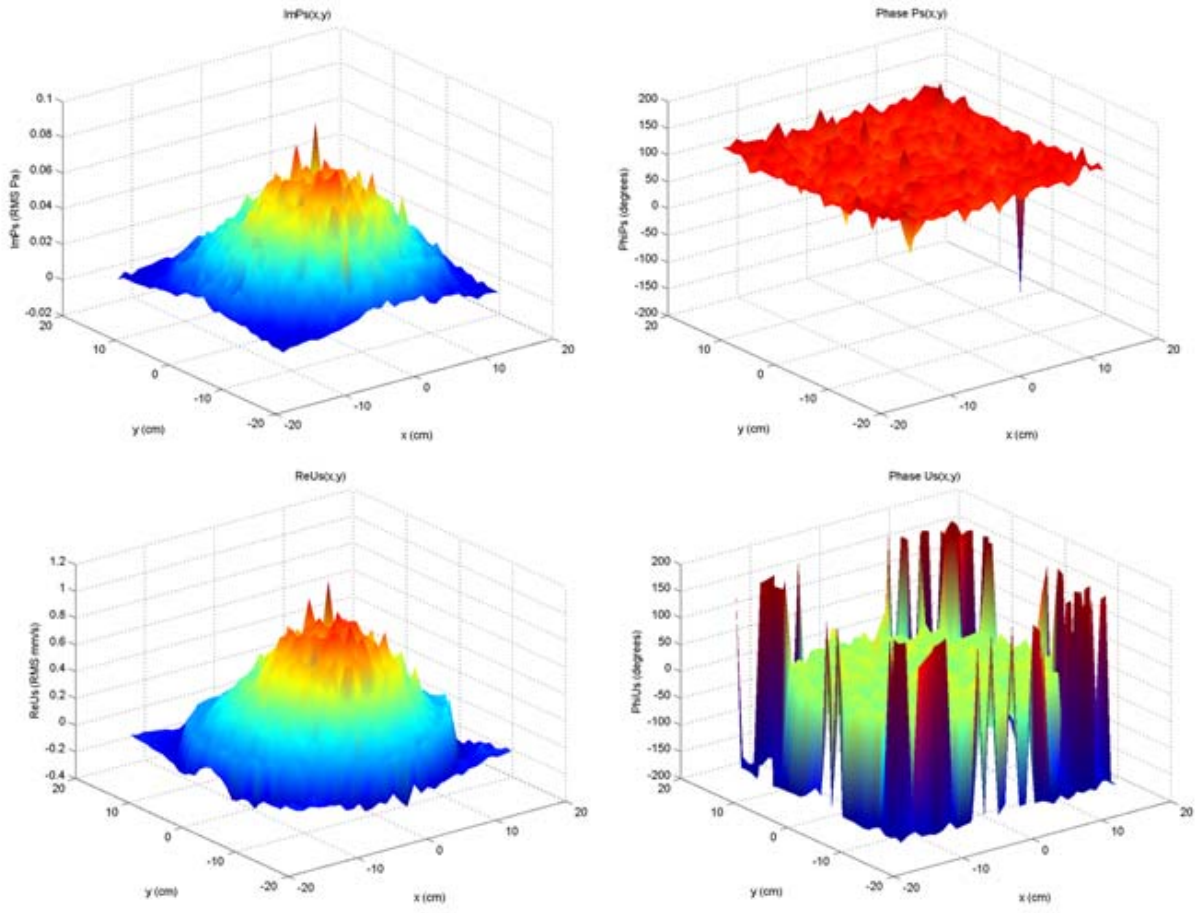

Figure 9: The (0,1) "breathing" mode of the drumhead. It is clear that the drumhead moves as a unit from both the left pictures, Re(P) and Im(U), as well as the fact that phase is roughly constant throughout the drumhead in both P and U.

For the (0,1) mode (above) it is clear that the drumhead is moving entirely in phase as a unit. This is evident in both plots of Im(p) and Re(u), as well as in the phase plots, which show both p and u to be at a constant phase. There are some unattractive spikes in the u data, which are likely a result of the microphone contacting the drumhead's rim.

The (0,2) mode (below) produces similar results, except with two coconcentric rings that are out of phase with one another. This can be seen in both the P, U plots, as well as in the 180° phase relation.

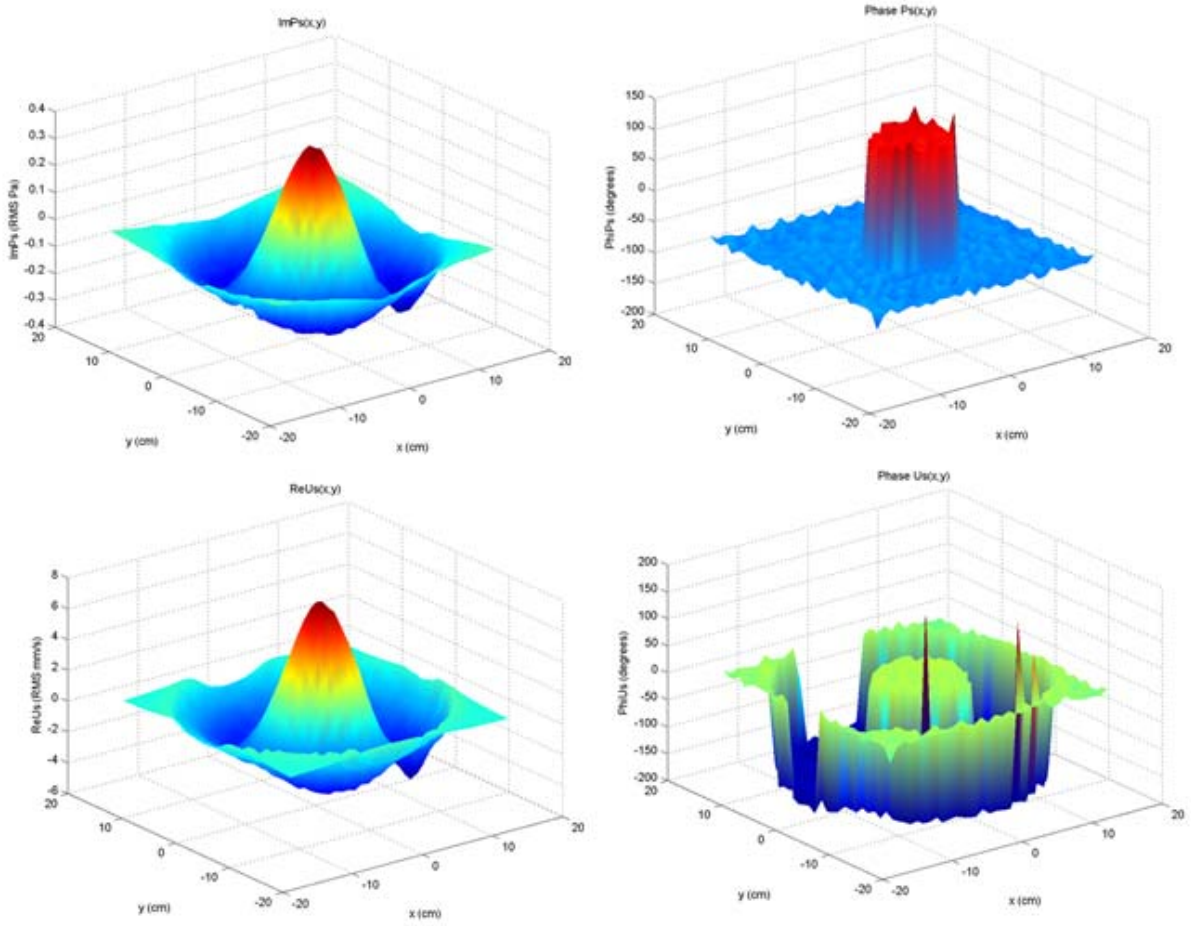

Figure 10: The (0,2) mode of the drumhead. Both the P, U diagram and phase diagram indicate that the drumhead moves as two out of phase concentric rings.

A preliminary scan of the (0,2) mode originally revealed an artifact of the drumhead being non-ideal membrane. As Fig. 11 shows, the vibrations of the drumhead were being damped. The damping edges run from the center to the drum's grommets, which are used to mount the drum to a stand. Raising the drumhead slightly off the grommets removed the damping effect. This was a testament to the sensitivity of the apparatus.

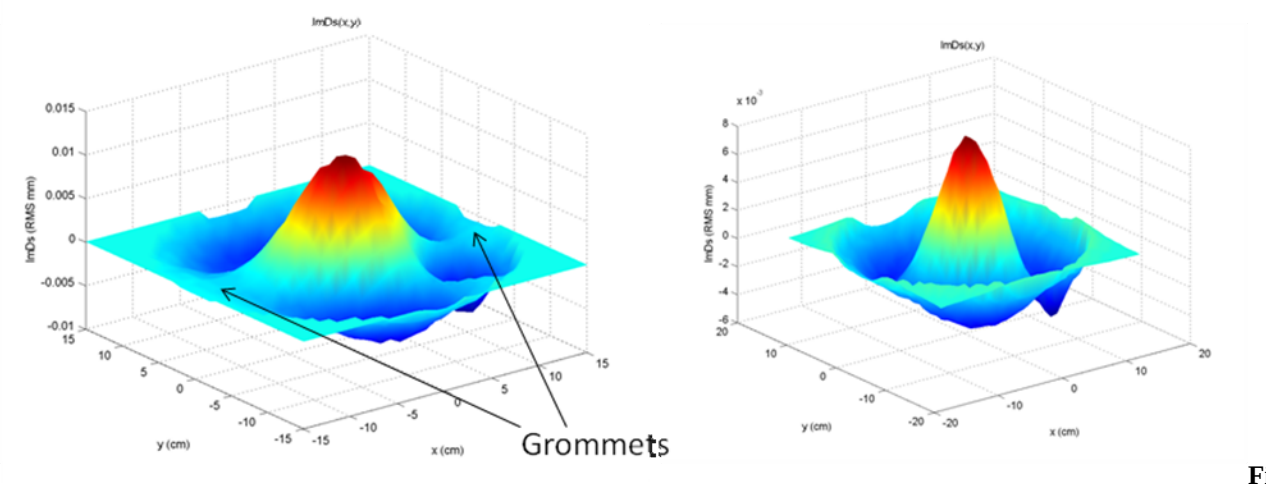

Figure 11: The effects of the drum's mounting. Grommets used to mount the drum to a stand caused damping over the drumhead (left). When the drum was raised slightly off of its supports, the damping was removed from the system (right).

Off axis modes were also scanned, by placing the magnet/coil configuration on an anti-node of the desired mode. Results are given in Fig. 12.

In the (1,0) mode (below), it is clear that the right and left side of the drum are 180° out of phase with each other as predicted by theory. In the u phase plot (bottom right), some of the phases on the right half of the plot (where phase is not zero) were recorded at near 180° while others near -180°. These two phases, physically speaking, are the same, though graphically they appear quite different.

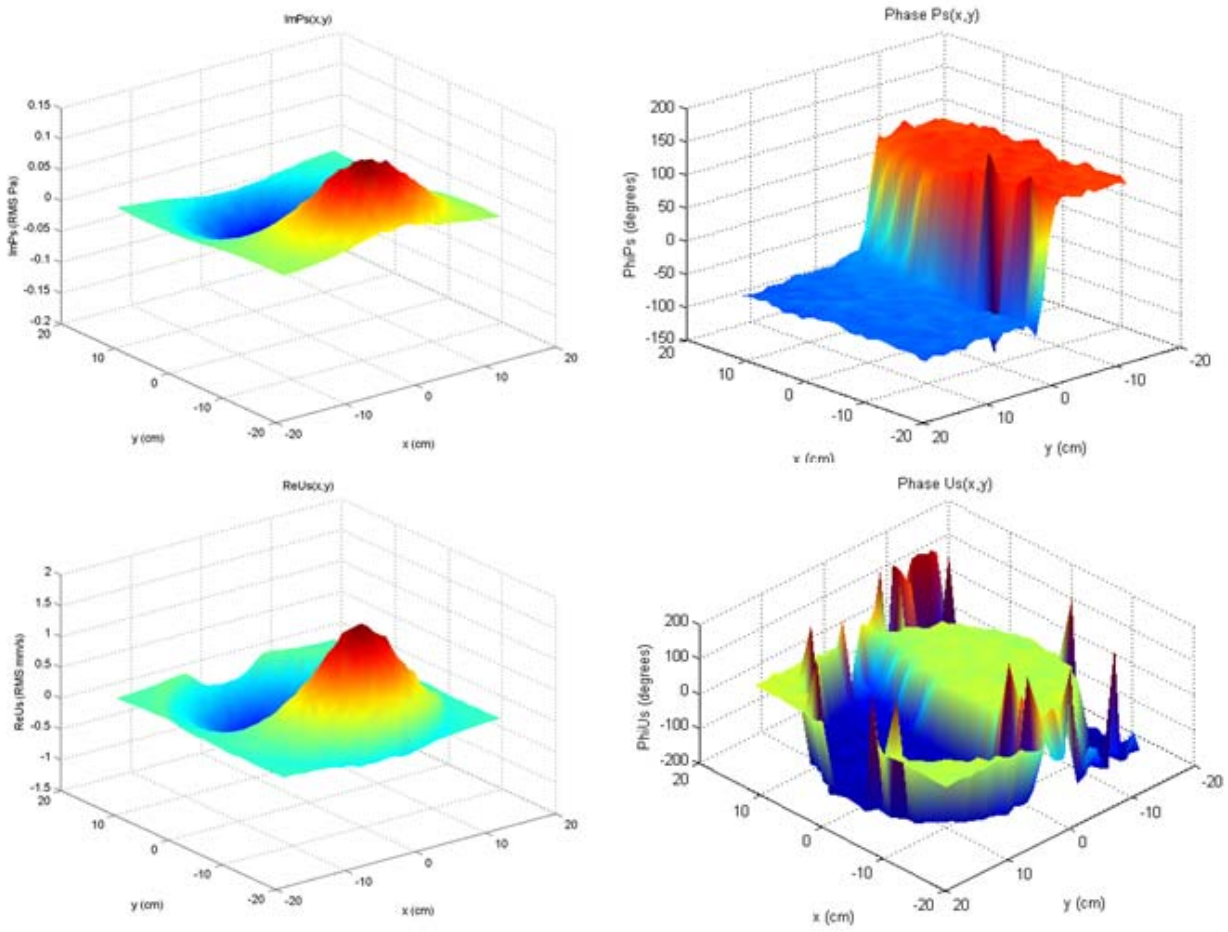

Figure 12: The (1,0) eigenmode. The left and the right side are 180° out of phase with each other. For the phase of u, it should be noted that on the right side, some points were found to have phases of 180° while others had -180°. In the complex plane, these two are equivalent, though graphically they appear to be quite different.

Though other modes were scanned, it is not necessarily fruitful to include them in the report. For those interested, all plots from scans taken will be available on the UIUC P199POM and P498POM websites in Adobe PDF form [9].

Discussions and Conclusions

This paper describes a phase-sensitive machine for acoustic holography. For several reasons it was tested by observing the eigenmodes of a vibrating drumhead. However, the apparatus was developed generally so that it can be used to map the sound field of any vibrating object.

The applications of a general acoustic holography machine range from geophysics to large scale auditorium and stadium design and instrument design. For instance, the damping observed by the drum's mounting is perhaps an effect the drum maker did not have the technology to observe. Acoustic holography is also a widely used in determining the internal contents of a rock [8], particularly in an effort to fine more oil. Though it is currently done only with magnitudes, the inclusion of phase may lead to a more fundamental standing of the acoustical properties of geological materials.

Acknowledgements

I would like to acknowledge, above all, my advisor Professor Steven Errede. I would also like to thank Nicole Pfeister (Purdue University) and Marguerite Brown (University of Chicago) for their shared workspace over the summer. This work was made possible through a grant from the Shell Oil Foundation through the Physics Department at the University of Illinois at Urbana-Champaign.

References

[1] ─ Sean F. Wu, Nassif Rayess, and Xiang Zhao, J. Acoust. Soc. Am. **109**, 2771-2779. (2001). "Visualization of acoustic radiation from a vibrating bowling ball."

[2] ─ T.D. Rossing, *The Physics of Musical Instruments* (1973).

[3] ─ Staffan Schedin, Per O. Gren, and Thomas D. Rossing, J. Acoust. Soc. Am.**103, 1217-1220.** (1998). "Transient wave response of a cymbal using double-pulsed TV holography"

[4] – Finn Jacobsen and Yang Liu, "Near field acoustic holography with particle velocity transducers," J. Acoust. Soc. Am. **118** (5), 2005.

[5] – S. Errede, "Near-Field Acoustic Holography," (unpublished).

[7] – D. Pignotti, "The Acoustic Impedance of a B-flat Trumpet," Senior Thesis, (unpublished)

[8] – Oscar Kelder and D.M.J. Smeulders, Geophysics **62**, 6, 1794-1796, (1997). "Observation of the Biot slow wave in water-saturated Nivelsteiner sandstone".

[9] – http://online.physics.uiuc.edu/courses/phys199pom/199pom_reu.html and http://online.physics.uiuc.edu/courses/phys498pom/498pom_reu.html